Chapter 14
Mössbauer Study of the Effect of Mechanical Activation on the Magnetic Properties of $PbFe_{0.5}Nb_{0.5}O_3$

S.P. Kubrin, I.P. Raevski, V.V. Stashenko, A.A. Gusev, V.P. Isupov, H. Chen, C.-C. Chou, D.A. Sarychev, V.V. Titov and S.I. Raevskaya

Abstract Mössbauer studies of $PbFe_{0.5}Nb_{0.5}O_3$ samples prepared by mechanical activation of PbO, Fe_2O_3 and Nb_2O_5 mixture and subsequent sintering at various temperatures T_S were performed. The room temperature Mössbauer spectra consist of two doublets (D1 and D2) for the samples with $T_S < 800$ °C and one doublet (D1) for the samples with $T_S > 800$ °C. The parameters of the doublet D1 correspond to Fe^{3+} in the octahedron environment. Doublet D2 has a lower isomer shift corresponding to Fe^{3+} with the coordination number 5 that indicates the presence of oxygen vacancies. Dependence of the temperature T_N of magnetic phase transition on T_S has a maximum at $T_S \approx 700$ °C. The effect of Fe^{3+}/Nb^{5+} ordering degree and oxygen deficiency on T_N is discussed.

14.1 Introduction

Ternary perovskite oxide $PbFe_{0.5}Nb_{0.5}O_3$ and its solid solutions exhibit high dielectric, piezoelectric, pyroelectric, electrostrictive responses [1–4]. Ceramics of these materials may be sintered at rather low temperatures (1050–1100 °C), and are prospective for many applications. As PFN contains a magnetic ion (Fe^{3+}) it

S.P. Kubrin · I.P. Raevski (✉) · V.V. Stashenko · D.A. Sarychev · V.V. Titov · S.I. Raevskaya
Faculty of Physics, Research Institute of Physics,
Southern Federal University, Rostov-on-Don, Russia
e-mail: igorraevsky@gmail.com

A.A. Gusev · V.P. Isupov
Institute of Solid State Chemistry and Mechanochemistry SB RAS,
Novosibirsk, Russia

H. Chen
University of Macau, Macau, China

C.-C. Chou
National Taiwan University of Science and Technology,
Taipei, Taiwan, China

I.A. Parinov et al. (eds.), *Advanced Materials*, Springer Proceedings in Physics 193, DOI 10.1007/978-3-319-56062-5_14

belongs to the currently very actively studied family of multiferroics. These materials possess simultaneously ferroelectric and magnetic orders [5–7]. On cooling PFN undergoes phase transitions from a cubic paraelectric phase to a tetragonal ferroelectric phase at $T_{CT} \approx 380$ K, then to a rhombohedral [8] (or monoclinic [9, 10]) ferroelectric phase at $T_{TR} \approx 360$ K and finally to a G-type antiferromagnetic (AFM) phase at $T_N \approx 150$ K [5, 6, 10]. In several works, magnetization loops were reported for ceramics and thin films of PFN and its analog $PbFe_{0.5}Ta_{0.5}O_3$ (PFT) as well as for their solid solutions with PZT [7, 11, 12]. As the T_N values of PFN, PFT and their solid solutions with $PbTiO_3$ (PT) and $PbZrO_3$ (PZ) are well below the room temperature [13–16] a possible origin of these room-temperature magnetic properties was supposed to be the formation of super-paramagnetic clusters [6, 7] and/or Fe spin clustering [11]. However in PFN-PT single crystals the super-antiferromagnetic and/or super-paramagnetic clusters were observed up to rather high temperatures well above the T_N, while the magnetization loops were observed only below ≈50 K [13]. Another possible explanation of these room-temperature magnetic properties is the presence of some small admixture of the ferromagnetic or ferrimagnetic phase, e.g. $PbFe_{12}O_{19}$, however its amount is below the detection limit of X-ray diffraction and Mössbauer spectroscopy [16, 17].

Until recently, there had been a belief that Fe and Nb in PFN are distributed over the lattice in a random fashion, but several observations now indicate that the Fe ions might segregate at the nanoscale level. Studies of ^{57}Fe Mössbauer spectra [18], as well as ^{93}Nb and ^{17}O NMR spectra [19] and magnetization [6] have led to the conclusion that PFN is a chemically inhomogeneous system and that long range AFM order forms in Fe-rich-Nb-poor regions while, a magnetic relaxor spin-glass like state below $T \approx 20$ K can arise from the Fe-poor-Nb-rich regions [6, 19]. These data are reinforced by the results of first principles calculations showing that Fe^{3+} and Nb^{5+} ions are distributed in the PFN lattice not randomly, but that they exhibit clustering [18]. Such clustering is actually a sort of local ordering changing the number of the nearest-neighbor Fe^{3+} ions and this fact, in particular, explains why the experimental values of T_N, for both PFN and PFT (≈150 K) are much lower than the calculated values of T_N for the case of random distribution of Fe^{3+} and Nb^{5+} (Ta^{5+}) ions in the lattice ($T_N \approx 300$ K) [20].

Such self-organization would be of great interest for applications if one could control it. Previously Li- doping was successfully used to change the compositional ordering degree of B-site cations in $PbB^{3+}_{0.5}B^{3+}_{0.5}O_3$ perovskites with B^{3+} = Sc, Yb; B^{5+} = Nb, Ta, [21]. Such ordering should decrease T_N as the number of the nearest-neighbor Fe^{3+} ions decreases. Indeed Li-doping was reported to decrease T_N value of PFN and PFT ceramics by ≈50 K [22].

However much more important is to increase T_N values, preferably up to room temperatures. Though linear-quadratic paramagnetoelectric effect in PFN ceramics is observed at room temperature and up to the ferroelectric Curie temperature $T_{CT} \approx$ 380 K, the value of this effect is several orders of magnitude lower that in the magnetic phase [23].

Some years ago there appeared a report that T_N value of the epitaxial PFN nanofilm is more than 50 K higher than that of the bulk samples [12]. Moreover in this film a remnant magnetization was observed up to room temperature, while in the bulk PFN single crystals it vanishes above ≈10–15 K [13]. These intriguing properties of PFN nanofilms seem to be due to the effect of epitaxial strain on the degree of Fe^{3+} and Nb^{5+} ions ordering. First-principles calculations support such possibility [24].

Recently we found out that T_N values of both PFN and PFT powders can be increased by 50–70 K by means of high-energy mechanical activation [25–27]. Such treatment is known to increase disorder of *B*-site cations in $PbB^{3+}_{0.5}B^{5+}_{0.5}O_3$ perovskites [28]. However the origin of the observed increase of T_N in mechanically activated multiferroics is not well understood yet.

The aim of the present study was a thorough study of Mössbauer spectra of mechanically activated PFN powders annealed at different temperatures in order to elucidate a correlation between T_N values and the environment of magnetic Fe^{3+} ions.

14.2 Experimental

PFN samples were fabricated from a stoichiometric mixture of high purity PbO, Fe_2O_3 and Nb_2O_5 powders. Mechanical activation was carried out using the high-energy planetary-centrifugal ball mill AGO-2 under a ball acceleration of 40 g. A mixture of powdered reagents (10 g) was placed into a steel cylinder together with 200 grams of steel balls, 8 mm in diameter. Activation was carried out for 15 min. After each five minutes of activation, the mill was stopped, the cylinders were opened, the powder was taken out and mixed, then it was put back into the cylinders for further mechanical activation. Besides the described above one-stage activation, the second batch of the powders was prepared by two-stage activation. At the first stage only Fe_2O_3 and Nb_2O_5 powders were activated for 15 min. At the second stage PbO was added and the resulting mixture was activated for 15 min. The samples for subsequent sintering were pressed at 1000 kg/cm^2 without a plasticizer. Sintering of the samples, placed into a closed alumina crucible, was carried out in an electric oven at different temperatures for 2 h. X-ray diffraction (XRD) studies were performed using DRON-3 diffractometer and Cu-K_α radiation. Transmission Mössbauer spectra of ^{57}Fe were measured with the aid of MS-1104EM rapid spectrometer and analyzed using the computer program SpectrRelax [29]. Mössbauer studies were carried out in the 12–320 K range using the closed-cycle helium cryostat-refrigerator Janis Ccs-850 (Cryogenics).

14.3 Results and Discussion

Figure 14.1 shows XRD patterns of mechanically activated stoichiometric mixture of PbO, Fe_2O_3 and Nb_2O_5 just after one-stage (a) and two-stage (b) activation. XRD patterns of both samples are very similar. One can see that using of AGO-2 high-energy planetary-centrifugal ball mill enables one to obtain practically pure perovskite phase of PFN after only 15 min of activation. It is worth noting that in the case of usual planetary or vibrating mills pure perovskite phase of PFN forms only after 20–30 h of activation [28, 30]. The diffraction reflexes of as-synthesized PFN are somewhat diffused, which seems to be caused by the small size of the particles formed. The mean size D of X-ray coherent scattering blocks, estimated using the Scherrer formula, appeared to be about 15–20 nm. Increase of the sintering temperature T_S leads to the sharpening of the diffraction reflexes (Fig. 14.1a, b, curves 2). This sharpening correlates with the increase of the D values up to ≈40 nm at T_S = 800 °C and 50–55 nm at higher sintering temperatures. However in the sample obtained by one-stage activation and sintered at 800 °C there is a substantial admixture of the parasitic pyrochlore phase (Fig. 14.1a, curve 2).

Figure 14.2 shows Mössbauer spectra of the same two samples. Both spectra are superposition of doublet and sextet. The doublet and sextet parameters are listed in Table 14.1. Parameters of sextet correspond to α-Fe_2O_3. The doublet is related to perovskite phase of PFN with admixture of $FeNbO_4$. The areas of doublet and sextet give the concentration of Fe ions in corresponding phases. Thus 25% of Fe^{3+} ions are related to PFN/$FeNbO_4$ phase in the sample (A). Similar ratio of the Fe_2O_3 and PFN/$FeNbO_4$ phases was reported for the stoichiometric mixture of PbO, Fe_2O_3 and Nb_2O_5 activated in SPEX 8000D vibrating mill for 20 h [30]. The doublet isomer shifts value correspond to Fe^{3+} state with coordination number 5 [31] and is lower than that for PFN single crystal (0.4 mm/s) [32]. The coordination number of Fe^{3+} ions in perovskites is 6. The reduction of coordination number is

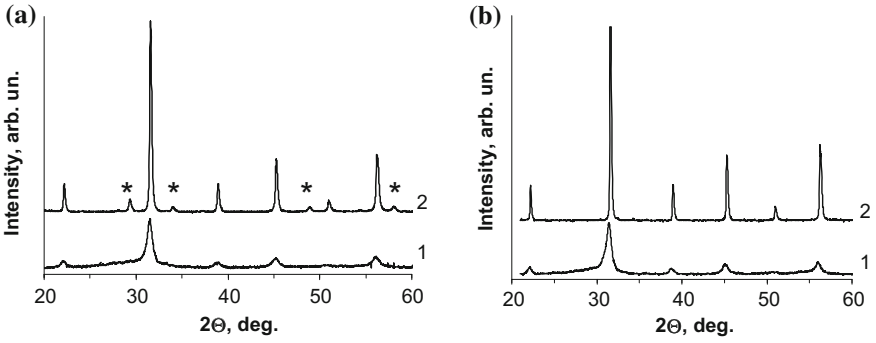

Fig. 14.1 X-ray diffraction patterns of mechanically activated stoichiometric mixture of PbO, Fe_2O_3 and Nb_2O_5 just after activation (*1*) and after sintering at 800 °C for 2 h (*2*): **a** one-stage activation; **b** two-stage activation; *asterisks mark* reflexes of the pyrochlore phase

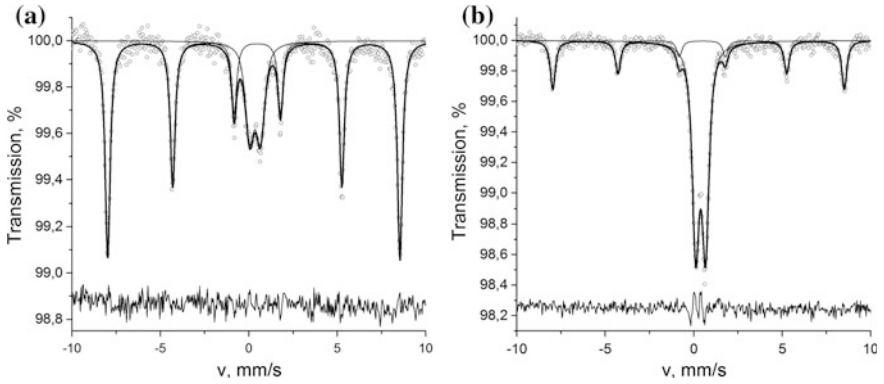

Fig. 14.2 Room-temperature ^{57}Fe Mossbauer spectra of mechanically activated stoichiometric mixture of PbO, Fe_2O_3 and Nb_2O_5. **a** One-stage activation. **b** Two-stage activation

Table 14.1 Parameters of room-temperature ^{57}Fe Mossbauer spectra of mechanically activated stoichiometric mixtures of PbO, Fe_2O_3 and Nb_2O_5

Preparation method	Spectrum component	$\delta \pm 0.02$, mm/s	$\Delta/\varepsilon \pm 0.02$, mm/s	$S \pm 2$, %	$H \pm 5$, kOe	$G \pm 0.02$, mm/s	χ^2
One-stage activation (Fig. 1a)	D	0.34	0.60	25		0.60	1.342
	S	0.37	−0.2	75	512	0.34	
Two-stage activation (Fig. 1b)	D	0.39	0.56	73		0.47	1.497
	S	0.38	−0.2	27	511	0.34	

D doublet, *S* sextet, δ isomer shift, Δ quadrupole splitting for paramagnetic component (doublet), ε quadrupole shift for sextet, *H* effective magnetic field on ^{57}Fe, *S* component area, *G* linewidth, χ^2 pearson's criterion

probably related to oxygen vacancies, which appear during mechanical activation. In addition, the quadrupole splitting value is higher than that for PFN single crystal (0.4 mm/s) because of high dispersion of the investigated mixture [33]. The doublet isomer shift value of the sample (B) is close to that for PFN single crystal and also corresponds to Fe^{3+} ions in the octahedron. The doublet quadrupole splitting value for sample (B) is lower than that for the sample (A). This fact may indicate the increase of the particle size. For further studies, the samples sintered from the powders fabricated by two-stage mechanical activation were used.

Mössbauer spectra of PFN samples sintered at different temperatures T_S from mechanically activated powders are present in Fig. 14.3. The spectra consist of one or two paramagnetic doublets. Their parameters are listed in Table 14.2. For some spectra, a Zeeman sextet is observed as well. The sextet parameters correspond to α-Fe_2O_3 admixture.

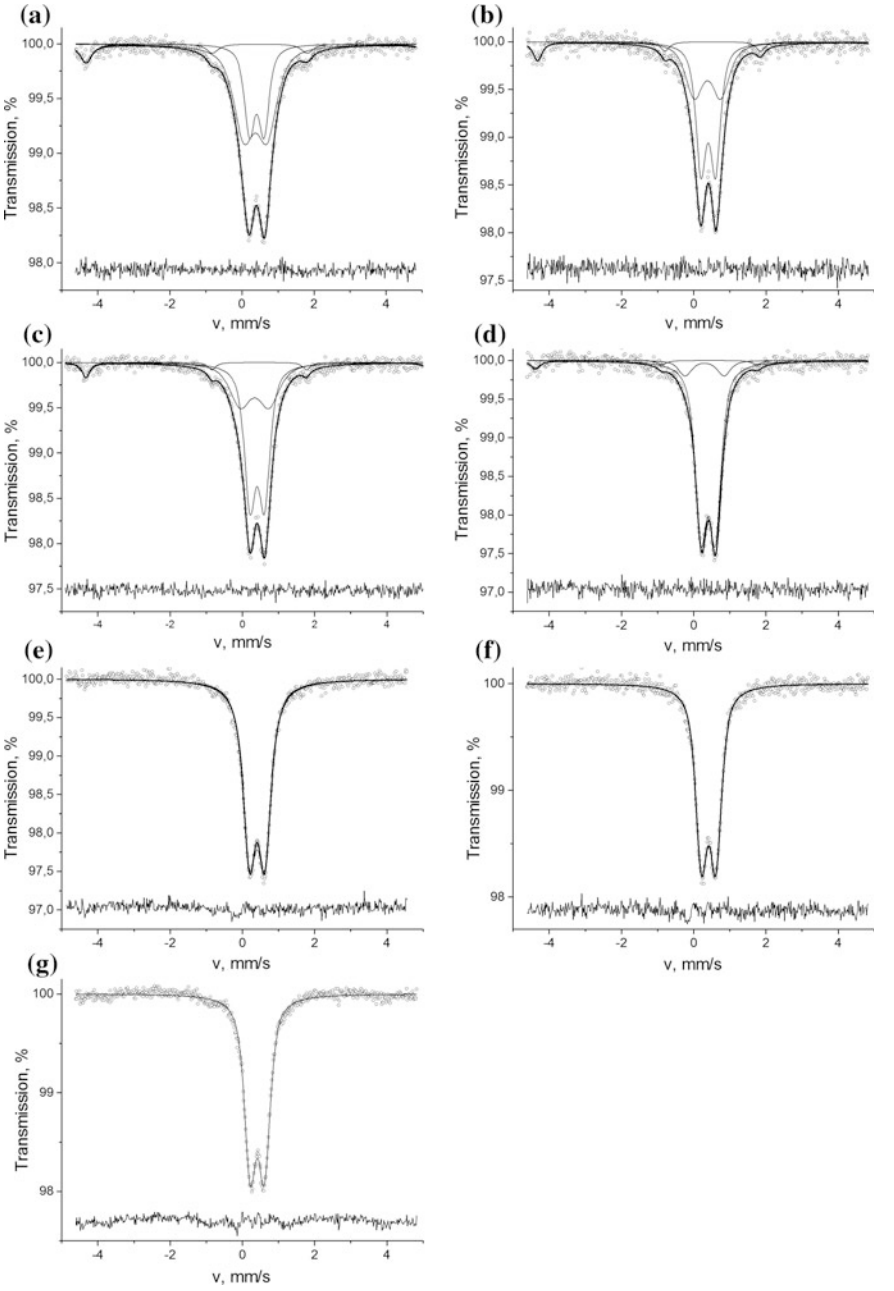

Fig. 14.3 Room temperature Mössbauer spectra of PFN samples sintered from mechanically activated powders at different temperatures: **a** T_s = 400 °C, **b** T_s = 500 °C, **c** T_s = 600 °C, **d** T_s = 700 °C, **e** T_s = 800 °C, **f** T_s = 1000 °C, **g** T_s = 1100 °C

Table 14.2 Parameters of room temperature Mössbauer spectra of PFN samples sintered from mechanically activated powders at different temperatures T_S

T_S, °C	Spectrum component	$\delta \pm 0.2$, mm/s	$\Delta/\varepsilon \pm 0.2$, mm/s	$A \pm 2$, %	$H \pm 5$, kOe	$G \pm 0.2$, mm/s	χ^2
400	D1	0.41	0.42	31		0.37	1.016
	D2	0.37	0.65	48		0.71	
	S1	0.30	−0.38	21	508	0.39	
500	D1	0.41	0.41	48		0.31	1.087
	D2	0.37	0.73	32		0.59	
	S1	0.30	−0.40	20	510	0.3	
600	D1	0.42	0.40	50		0.37	0.953
	D2	0.34	0.72	36		0.72	
	S1	0.30	−0.34	14	508	0.3	
700	D1	0.41	0.39	73		0.37	1.121
	D2	0.36	0.86	17		0.66	
	S1	0.30	−0.26	10	509	0.3	
800	D1	0.41	0.42	100		0.42	1.463
1000	D1	0.41	0.40	100		0.39	1.150
1100	D1	0.41	0.39	100		0.39	1.809

D doublet, *S* sextet, δ isomer shift, Δ quadrupole splitting for paramagnetic component (doublet), ε quadrupole shift for sextet, *H* effective magnetic field on ^{57}Fe, *A* component area, *G* linewidth, χ^2 Pearson's criterion

The spectra of the samples with T_S = 400–700 °C are a superposition of two doublets D1 and D2. The D1 parametres correspond to Fe^{3+} ions in octahedron and are close to parametres of PFN synthesized by conventional solid-phase reactions route [18]. The doublet D1 is present in the spectra of all the samples. The quadruple splitting is a consequence of the composition disorder in *B*-sublattice of PFN. In contrast to this, Mössbauer spectrum of the highly ordered (in the rock-salt manner) $PbFe_{1/2}Sb_{1/2}O_3$ perovskite appears to be a singlet at room temperature [34]. The second doublet D2 has an isomer shift value ≈0.36–0.37 mm/s that is lower than that for D1. The reduction of the isomer shift value indicates the lowering of coordination number due to the presence of oxygen vacancies. The doublet D2 quadruple splitting value is higher than that of D1, showing the presence of large crystallographic distortions in close environment of Fe^{3+} ions. The oxygen vacancies and distortions are probably related to the appearance of crystallographic shear planes during mechanical activation. The line broadening of D2 may be also due to the inhomogeneity of the environment of Fe^{3+} ions.

Figure 14.4 shows the dependence of the Mössbauer spectra component's area on T_S. The D2 area decreases as T_S grows. Thus the oxygen vacancies concentration decreases with the increase of T_S. In addition, the α-Fe_2O_3 impurity disappears when T_S exceeds 700 °C. The isomer shift and quadrupole splitting dependencies on T_S are present in Figs. 14.5 and 14.6. One can see that the isomer shift does not

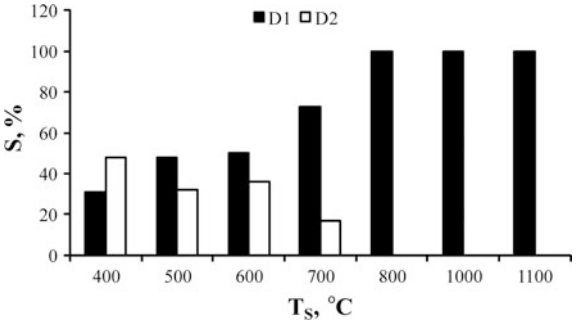

Fig. 14.4 Dependence of Mössbauer spectra doublets' area S on T_S for PFN samples sintered from mechanically activated powders at different temperatures T_S

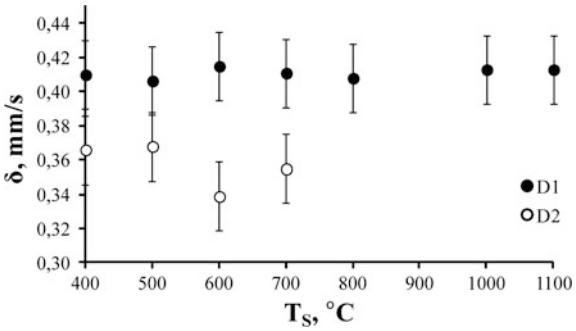

Fig. 14.5 Dependence of Mössbauer spectra isomer shifts on T_S for PFN samples sintered from mechanically activated powders at different temperatures T_S

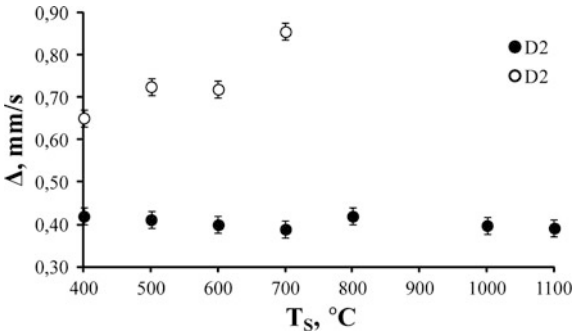

Fig. 14.6 Dependence of Mössbauer spectra quadruple splitting on T_S for PFN samples sintered from mechanically activated powders at different temperatures T_S

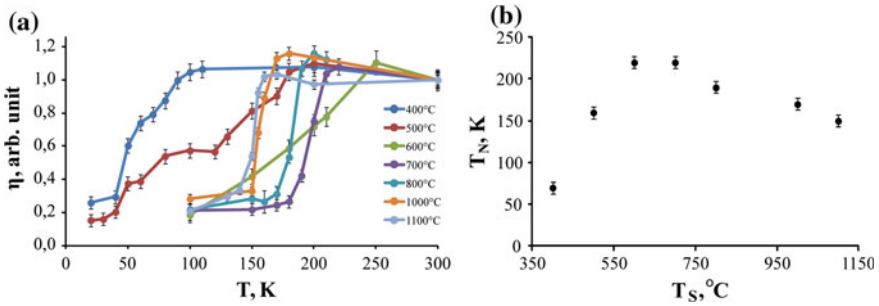

Fig. 14.7 **a** Temperature dependencies of η-maximal intensity of doublet in Mössbauer spectrum related to its value at 300 K for PFN samples, sintered from mechanically activated powders at different temperatures T_S; **b** magnetic phase transition temperature dependence on T_S for PFN samples sintered from mechanically activated powders at different temperatures T_S

change as T_S increases. The quadrupole splitting of D2 increases with T_S indicating the growth of crystallography distortions around Fe^{3+} ions corresponding to D2.

For estimation of magnetic phase transition temperature T_N, the method of temperature scanning was used. The essence of temperature scanning is measuring of Mössbauer spectrum line intensity in the course of sequential decreasing of the temperature. When magnetic ordering appears, the paramagnetic doublet transforms into Zeeman sextet, which is accompanied by a dramatic decrease of the line intensity. The temperature dependencies of Mössbauer spectrum intensity η, related to its value at 300 K for PFN ceramic samples, sintered at different temperatures from mechanically activated powders, are present in Fig. 14.7a. The abrupt drop of $\eta(T)$ curve corresponds to T_N value.

One can see from Fig. 14.7a that the samples sintered at T_s = 400–600 °C have diffused magnetic phase transitions in a wide temperature range. For the samples sintered at higher T_S, magnetic phase transitions temperature range is much more narrower. This may come from the lowering of inhomogeneity in the environment of Fe^{3+} ions and growth of grain size. Figure 14.7b shows the T_N versus T_S dependence for PFN samples studied. The T_N value grows up to ≈220 K as T_S increases from 400 up to 700 °C and on further increase of sintering temperature T_N gradually lowers down to ≈150 K, i.e. to the value typical of PFN single crystal. The uprising part of $T_N(T_S)$ dependence corresponds to T_S range, where the D2 area decreases.

The magnetic structure in perovskites comes from 180° superexchange between Fe^{3+} ions. So the T_N value is determined by the number of Fe^{3+}–O^2–Fe^{3+} links [35]. This number depends on the degree of compositional ordering of Fe^{3+} and Nb^{5+} ions. Namely, the Fe^{3+}–O^2–Fe^{3+} links number increases, when the compositional ordering degree lowers. In addition, oxygen vacancies also reduce the number of Fe^{3+}–O^2–Fe^{3+} links. Thus, the T_N growth with T_S in the 400–600 °C range coincides with decrease of oxygen vacancies' concentration. The largest values of T_N in the samples sintered in the 650–800 °C range are probably explained by growing of grain size as well as by compositional disorder stimulated by mechanical activation.

Decrease of T_N values in the samples sintered at $T_S > 800$ °C comes from appearing of the regions with local compositional ordering of Fe^{3+} and Nb^{5+}.

14.4 Summary

In PFN ceramics sintered from mechanically activated powders dependence of the temperature T_N of magnetic phase transition on sintering temperature T_S has a maximum at $T_S \approx 700$ °C. The low T_N value of the samples having lower T_S is likely to be connected with a small size of $PbFe_{0.5}Nb_{0.5}O_3$ particles, presence of $FeNbO_4$ admixture as well as with oxygen deficiency. In the samples, sintered at 600–700 °C, T_N achieves the maximal value and slowly decreases to 150 K in the samples with higher T_S. The T_N value in oxides depends on the number of Fe–O–Fe links, which in turn correlates with Fe^{3+}/Nb^{5+} cation ordering degree and oxygen deficiency. Thus, it seems that in the samples with $T_S \leq 700$ °C, the clusters with low cation ordering degree are present. The oxygen deficiency in such samples is probably related to the appearance of crystallographic shear planes during mechanical activation.

Acknowledgements This work was partially supported by Ministry of Education and Science of the Russian Federation (Research project No. 3.5346.2017/BP), Russian Foundation for Basic Research (project 17–03–01293_a) and Research Committee of the University of Macau under Research & Development Grant for Chair Professor No RDG007/FST-CHD/2012.

References

1. I.P. Raevskii, S.T. Kirillov, M.A. Malitskaya, V.P. Filippenko, S.M. Zaitsev, L.G. Kolomin, Inorg. Mater. **24**, 217 (1988)
2. YuN Zakharov, S.I. Raevskaya, A.G. Lutokhin, V.V. Titov, I.P. Raevski, V.G. Smotrakov, V. V. Eremkin, A.S. Emelyanov, A.A. Pavelko, Ferroelectrics **399**, 20 (2010)
3. D. Bochenek, P. Kruk, R. Skulski, P. Wawrzała, J. Electroceram. **26**, 8 (2011)
4. E.I. Sitalo, I.P. Raevski, A.G. Lutokhin, A.V. Blazhevich, S.P. Kubrin, S.I. Raevskaya, Y.N. Zakharov, M.A. Malitskaya, V.V. Titov, I.N. Zakharchenko, IEEE Trans. Ultrason. Ferroelectr. Freq. Contr. **58**, 1914 (2011)
5. D.I. Khomskii, J. Magn. Magn. Mater. **306**, 1 (2006)
6. W. Kleemann, V.V. Shvartsman, P. Borisov, A. Kania, Phys. Rev. Lett. **105**, 257202 (2010)
7. R. Blinc, P. Cevc, A. Zorko, J. Holc, M. Kosec, Z. Trontelj, J. Pirnat, N. Dalal, V. Ramachandran, J. Krzystek, J. Appl. Phys. **101**, 033901 (2007)
8. K.H. Ehses, H.Z. Schmid, Kristallography **162**, 64 (1983)
9. W. Bonny, M. Bonin, Ph Sciau, K.J. Schenk, G. Chapuis, Solid State Commun. **102**, 347 (1997)
10. S.P. Singh, S.M. Yusuf, S. Yoon, S. Baik, N. Shin, D. Pandey, Acta Mater. **58**, 5381 (2010)
11. D.A. Sanchez, N. Ortega, A. Kumar, G. Sreenivasulu, R.S. Katiyar, J.F. Scott, D.M. Evans, M. Arredondo-Arechavala, A. Schilling, J.M. Gregg, J. Appl. Phys. **113**, 074105 (2013)
12. W. Peng, N. Lemee, M. Karkut, B. Dkhil, V. Shvartsman, P. Borisov, W. Kleemann, J. Holc, M. Kosec, R. Blinc, Appl. Phys. Lett. **94**, 012509 (2009)

13. V.V. Laguta, M.D. Glinchuk, M. Maryško, R.O. Kuzian, S.A. Prosandeev, S.I. Raevskaya, V. G. Smotrakov, V.V. Eremkin, I.P. Raevski, Phys. Rev. B. **87**, 064403 (2013)
14. I.P. Raevski, S.P. Kubrin, S.I. Raevskaya, S.A. Prosandeev, M.A. Malitskaya, V.V. Titov, D. A. Sarychev, A.V. Blazhevich, I.N. Zakharchenko, IEEE Trans. Ultrason. Ferroelectr. Freq. Contr. **59**, 1872 (2012)
15. I.P. Raevski, S.P. Kubrin, V.V. Laguta, M. Marysko, H. Chen, S.I. Raevskaya, V.V. Titov, C.-C. Chou, A.V. Blazhevich, E.I. Sitalo, D.A. Sarychev, T.A. Minasyan, A.G. Lutokhin, YuN Zakharov, L.E. Pustovaya, I.N. Zakharchenko, M.A. Malitskaya, Ferroelectrics **475**, 20 (2015)
16. I.P. Raevski, V.V. Titov, M.A. Malitskaya, E.V. Eremin, S.P. Kubrin, A.V. Blazhevich, H. Chen, C.-C. Chou, S.I. Raevskaya, I.N. Zakharchenko, D.A. Sarychev, S.I. Shevtsova, J. Mater. Sci. **49**, 6459 (2014)
17. A.A. Gusev, S.I. Raevskaya, V.V. Titov, V.P. Isupov, E.G. Avvakumov, I.P. Raevski, H. Chen, C.-C. Chou, S.P. Kubrin, S.V. Titov, M.A. Malitskaya, D.A. Sarychev, V.V. Stashenko, S.I. Shevtsova, Ferroelectrics **496**, 231 (2016)
18. I.P. Raevski, S.P. Kubrin, S.I. Raevskaya, D.A. Sarychev, S.A. Prosandeev, M.A. Malitskaya, Phys. Rev. B. **85**, 224412 (2012)
19. V.V. Laguta, J. Rosa, L. Jastrabik, R. Blinc, P. Cevc, M. Zalar, B. Remskar, S.I. Raevskaya, I. P. Raevski, Mater. Res. Bull. **45**, 1720 (2010)
20. S. Nomura, H. Takabayashi, T. Nakagawa, Jpn. J. Appl. Phys. **7**, 600 (1968)
21. I.P. Raevski, VYu. Shonov, M.A. Malitskaya, E.S. Gagarina, V.G. Smotrakov, V.V. Eremkin, Ferroelectrics **235**, 205 (1999)
22. I.P. Raevski, S.P. Kubrin, S.I. Raevskaya, V.V. Stashenko, D.A. Sarychev, M.A. Malitskaya, M.A. Seredkina, V.G. Smotrakov, I.N. Zakharchenko, V.V. Eremkin, Ferroelectrics **373**, 121 (2008)
23. V.V. Laguta, A.N. Morozovska, E.I. Eliseev, I.P. Raevski, S.I. Raevskaya, E.I. Sitalo, S.A. Prosandeev, L. Bellaiche, J. Mater. Sci. **51**, 5330 (2016)
24. S.A. Prosandeev, I.P. Raevski, S.I. Raevskaya, H. Chen, Phys. Rev. B. **92**, 220419(R) (2015)
25. A.A. Gusev, S.I. Raevskaya, V.V. Titov, E.G. Avvakumov, V.P. Isupov, I.P. Raevski, H. Chen, C.-C. Chou, S.P. Kubrin, S.V. Titov, M.A. Malitskaya, A.V. Blazhevich, D.A. Sarychev, V.V. Stashenko, S.I. Shevtsova, Ferroelectrics **475**, 41 (2015)
26. A.A. Gusev, S.I. Raevskaya, V.V. Titov, V.P. Isupov, E.G. Avvakumov, I.P. Raevski, H. Chen, C.-C. Chou, S.P. Kubrin, S.V. Titov, M.A. Malitskaya, D.A. Sarychev, V.V. Stashenko, S.I. Shevtsova, Ferroelectrics **496**, 231 (2016)
27. A.A. Gusev, S.I. Raevskaya, I.P. Raevski, V.P. Isupov, E.G. Avvakumov, S.P. Kubrin, H. Chen, V.V. Titov, T.A. Minasyan, C.-C. Chou, S.V. Titov, M.A. Malitskaya, Ferroelectrics **496**, 250 (2016)
28. X. Gao, J. Xue, J. Wang, Mater. Sci. Eng. B **99**, 63 (2003)
29. M.E. Matsnev, V.S. Rusakov, AIP Conf. Proc. **1489**, 178 (2012)
30. D. Bochenek, G. Dercz, D. Oleszak, Arch. Metall. Mater. A. **56**, 1015 (2011)
31. F. Menil, J. Phys. Chem. Solids **46**, 763 (1985)
32. S.P. Kubrin, S.I. Raevskaya, S.A. Kuropatkina, D.A. Sarychev, I.P. Raevski, Ferroelectrics **340**, 155 (2006)
33. W. Kundig, H. Bommel, G. Constabaris, R.H. Lindquist, Phys. Rev. **142**, 327 (1966)
34. I.P. Raevski, N.M. Olekhnovich, A.V. Pushkarev, Y.V. Radyush, S.P. Kubrin, S.I. Raevskaya, M.A. Malitskaya, V.V. Titov, V.V. Stashenko, Ferroelectrics **444**, 47 (2013)
35. J.B. Goodenough, *Magnetism and Chemical Bond.* (Interscience Publisher, a division of Wiley, New York, London, 1963), 393 pp